ARTICLES

Ion Yields of Thin MALDI Samples: Dependence on Matrix and Metal Substrate and Implications for Models

R. Knochenmuss,* G. McCombie, and M. Faderl

Novartis Institutes of Biomedical Research, 4002 Basel, Switzerland

Received: July 26, 2006; In Final Form: September 20, 2006

Thin MALDI samples can perform differently than thicker samples, on metal substrates. Divergent results and models for the effect have been presented. Positive and negative yields are investigated here for three matrixes (2,5-dihydroxybenzoic acid (DHB), sinapinic acid, and α-cyano 4-hydroxycinnamic acid) on stainless steel and gold substrates. Samples were electrosprayed for uniformity and thickness control and imaged across a metal−metal boundary. Thin sample enhancement is found in both polarities for all three matrixes on a steel substrate. On gold, only α-cyano-4-hydroxycinnamic acid shows enhancement. These and earlier data are used to evaluate two models. The first is based on one-photon photoelectron emission from the metal; the second one, on two-photon matrix ionization at the metal interface. The surface-enhanced matrix photoionization model best fits the evidence, including the fluence dependence of electron emission from DHB on steel.

Introduction

Reports have recently appeared regarding the ultraviolet (UV) MALDI ion yield as a function of metal substrate, for thin samples. Studies performed in the magnet of an FT-ICR mass spectrometer[1−4] reported decreased positive ion yield from dried-drop samples on stainless steel vs thick samples. The decrease was less pronounced on gold substrates. The samples were sequentially prepared dried drops, which did not have a uniform thickness or homogeneous surface coverage. Spatially averaged spectra were reported.

A study performed on a delayed-extraction time-of-flight (TOF) instrument[5] reported the inverse: significantly increased positive ion yield on stainless steel and a smaller enhancement on gold. These conclusions were based on MALDI images, which represent hundreds or thousands of independent spectra. The samples were electrosprayed[6,7] on a stainless steel substrate half-coated with gold and were spatially uniform.

Since the observations differ, so also do the interpretations. The earlier work[3,4] proposes that electrons are emitted in a one-photon process from partially matrix-covered metal. This should be more efficient than in bulk matrix, where the process is energetically three-photon.[8,9] Because of the low order of the process, photoelectrons may be copious. They are then captured by neutral matrix molecules, the probability of which has a marked peak at low energy,[10] although this broadens at higher temperature.[11,12] The energy of photoelectrons emitted from the metal interface varies with the work function of the metal and determines the amount of matrix anions formed. Excess anion density in the plume decreases the positive yield by neutralization. This model is here denoted the photoelectron capture model (PEC; Figure 1). It bears superficial similarity to the "lucky survivors" MALDI model[13] but is a surface effect, whereas the survivors model is concerned only with bulk MALDI matrix.

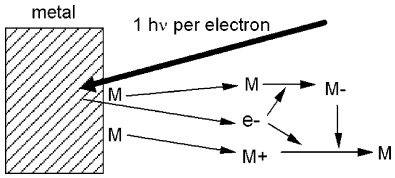

Figure 1. Sketch of the photoelectron capture (PEC) model for one-photon ionization of the metal surface with adsorbed matrix (M). Matrix interaction with the metal is proposed to lower the work function so much that it falls below the photon energies of typical MALDI UV lasers. Electrons are ejected directly from the metal and may be captured to create matrix anions. Positive ion yield is predicted to be reduced compared to a thick sample, due to the excess of negative charge.

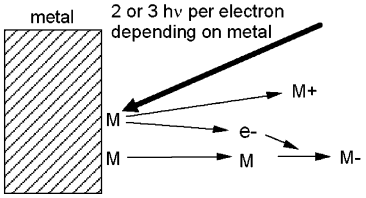

Figure 2. Sketch of the surface enhancement model (SEM) for two-photon ionization of matrix on a metal surface. If the matrix−metal interaction is favorable, surface matrix ionization is energetically two-photon (stainless steel), while it remains three-photon in the bulk and on unfavorable metals with a lower Fermi level (gold). Each ionization event generates a matrix cation and an electron which may be captured from matrix anions. There is no excess negative charge. See Figure 4 for a more detailed diagram of the matrix−metal interaction.

The second model[5,14] is denoted the surface enhancement model (SEM; Figure 2), since increased rather than decreased signal is found. In this model, surface matrix is readily photoionized on some metals in a two-photon process, while on others it remains three-photon, as for bulk matrix. The metal

* To whom correspondence should be addressed. Telephone: ++41 61 324 4541. Fax: ++41 61 324 8868. E-mail: richard.knochenmuss@novartis.com.

10.1021/jp064760t CCC: $33.50
Published on Web 11/02/2006

dependence enters via the relative positions of the Fermi level and the LUMO of the adsorbed matrix, which determine the surface states which can arise. In the SEM, equivalent amounts of positive and negative charge are emitted, so increased photoionization results in increased yield in both polarities. Positive ions are formed directly, but negative ion yield depends on the sample thickness compared to the mean electron capture distance of the matrix material.

Several aspects of these models are testable. First, the PEC predicts reduction in positive ion signal on certain metals,[3] while the SEM predicts either enhancements or no effect (depending on matrix and metal).[5] Second, the PEC has been reported for a few MALDI matrix materials, but as yet makes no explicit prediction of which matrixes will show a strong effect. In contrast the SEM is based on a physical picture which allows prediction of the matrixes for which enhancement can be expected, and on which metals. Third, the PEC predicts that the negative ion spectrum changes dramatically (in intensity and in ions observed) vs metal substrate, based on electron capture probability.[4] The SEM predicts that the negative spectrum is enhanced in the same way as the positive, but does not predict major changes in the ions observed. Fourth and finally, the PEC predicts a linear dependence of photoelectron yield on laser intensity. The SEM predicts a nonlinear functional form which does not have a simple power dependence.

Before comparing the models and data, it is useful to consider briefly the concept of a "thin" sample in MALDI. By this we mean the substrate must have a direct role in ionization (as opposed to indirect effects such as influencing the matrix crystallization process). Given the absorption cross-sections of typical matrixes, on the order of 10^{-17} cm^2 at 355 nm,[15−17] this means thicknesses of at most a few 100 nm. Within such distances, some laser light will reach the surface. A trivial effect of this is that the effective laser intensity near the surface can be enhanced by reflected light. Larger, nontrivial, effects can appear for the last few monolayers of the matrix. To the extent that these are within the electron tunneling distance of the metal, and therefore have some wave function overlap with it, fundamental changes in photoionization behavior are possible. These interactions are of primary interest here.

Experimental Section

The electrospray deposition system used a CTC-PAL syringe autosampler (Zwingen, Switzerland) to pump the analyte/matrix solution. After aspiration of a 10 μL sample solution, 8.5 μL was ejected to flush the tubing and spray needle. This spray was pneumatically assisted to prevent the formation of droplets that could leave residue on the needle. The MALDI spots or traces were sprayed at a rate of 30 nL/s, with no pneumatic assistance. The needle was positioned 6 mm above the target plate, and a potential of +5 kV was applied. The target plate was moved manually between depositions but could be moved continuously by a motorized translation stage during deposition. Unless otherwise noted, the sprayed solutions were as follows: 2,5-dihydroxybenzoic acid (DHB), 160 mM in 70:30 methanol/water; sinapinic acid (SA), 45 mM in 70:30 methanol/water; 4-hydroxycinnamic acid (HCCA), 53 mM in 80:20 methanol/water.

All mass spectra were measured on a Voyager-DE STR MALDI TOF instrument, (Applied Biosystems, Framingham, MA). Reflectron mode and an acceleration voltage of 20 kV were used. The acceleration pulse delay was 175 ns. The 355 nm laser intensity was around 100 units over the apparent threshold value. The fluences for all experiments were within the normal range for typical MALDI experiments.

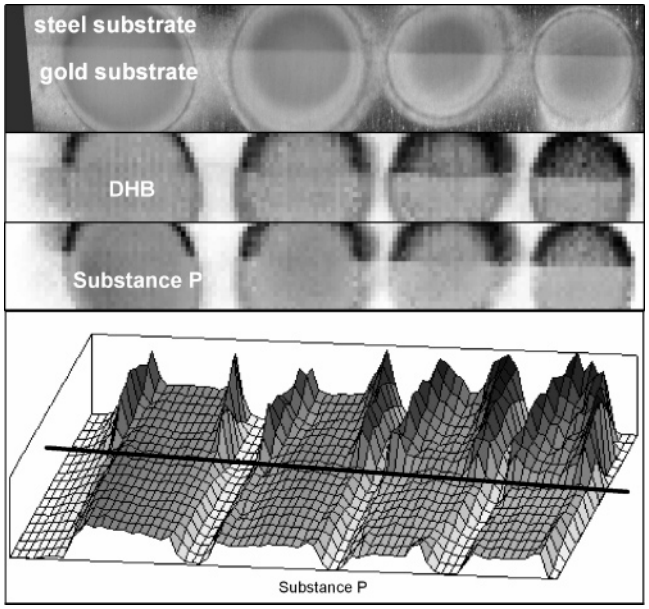

Figure 3. Electrosprayed DHB MALDI spots on a stainless steel substrate which has been half-coated with 35 nm gold. The upper image is an optical micrograph of the spots before MALDI imaging. The thinnest spot is on the right; the thickest, on the left. The range is approximately 200−3000 nm mean thickness. The lower images were extracted from the MALDI imaging data cubes (100 μm raster step size) for the indicated protonated positive ions. Darker pixels indicate stronger signal. The substantial signal enhancement of thin sample regions on steel is apparent, as is the much weaker effect on gold. The sprayed solution was substance P, 180 μM, with matrix 50 mg/mL (325 mM) DHB in 48.5:50:1.5 chloroform/methanol/water. Adapted from ref 5.

The sample plates were made from 1 mm magnetic stainless steel, shaped to fit into a standard Voyager sample holder. The plates were coated over half the surface with 40 nm of gold in a sputter coater equipped with a microbalance thickness sensor (Polaron, Quorum Technologies, Newhaven, U.K.).

The MALDI instrument has been adapted for fast mass spectrometric imaging.[18] For every image point, 30 shots (mass spectra) were typically averaged. The raster step size was 100−400 μm. The images were directly analyzed using Igor Pro (Wavemetrics, Lake Oswego, OR). In some cases analyte was present in the matrix, which can be described as true matrix-assisted laser desorption/ionization, at least for the analyte. In others, only matrix was present, which might rigorously be descibed as merely LDI. However, we retain the term MALDI in all cases, since these materials are of general interest only due to their application in this field.

Results and Discussion

Positive Ion Yield as a Function of Matrix and Metal. Initial reports of decreased positive ion yield on metal substrates compared to thick samples or nonmetallic substrates[1−4,19] led to questions about the description of heterogeneous dried-drop samples as thick or thin. These were shown to be much less uniform than electrosprayed samples.[5] In that work increased, not decreased, positive ion signal was observed for thin DHB matrix on stainless steel (SS), as shown in Figure 3. A smaller enhancement was also found for thin DHB on a 35 nm gold layer sputter-coated onto the SS.

The increase of positive matrix and analyte signals was localized by drilling experiments at the matrix−metal boundary.[5] Since thinner samples are easily ablated to the metal with a moderate number of laser shots, they give strong signal over

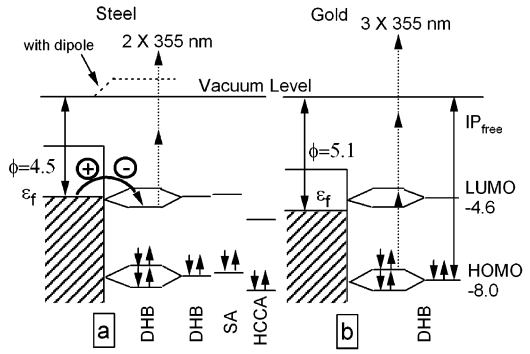

Figure 4. Simplified diagram of MALDI matrixes adsorbed on the surface of stainless steel (a) and gold (b). The vertical axis is in electronvolts vs the vacuum level. The metal conduction band is on the left and free matrixes on the right. The ionization potential and LUMO energy for DHB are from ref 8. The IPs of SA and CCA are from ref 25, and the LUMO positions are estimated from the absorption spectra.[15,26] DHB on the metal surface is shown with (exaggerated) level splittings due to interaction with the metal. If the Fermi level is high enough, the LUMO of the adsorbed molecules can be populated, making two-photon ionization possible. For lower lying Fermi levels, ionization remains energetically three-photon, and hence less efficient. The vacuum level shift due to the surface dipole increases the required ionization energy[20] but is more than compensated for by the higher energetic position of the LUMO-derived surface state.

the entire area. In contrast, ablation is complete, and enhancement observed, only at the thinner edge of thick samples.

The SEM mechanism predicts that ionization enhancement is a function of the energetic location of matrix electronic levels with respect to the conduction band of the metal. Figure 4 shows if the matrix LUMO lies below the metal Fermi level, some charge transfer can occur from metal to adsorbed matrix. The coefficient of the LUMO in the mixed surface state reflects the degree of charge transfer and will not be large for the nonbonding adsorption expected here. Only a fractional electron charge then resides on surface DHB molecules. This dipole increases the surface vacuum level,[20] as shown, but this is more than compensated for by the position of the mixed state, which is far higher in energy than the HOMO-derived states. Note that we have neglected any condensed-phase ionization potential (IP) reductions, since only small decreases have been observed in clusters,[9] and since ionization of thick DHB samples is less facile, and hence not in the two-photon range. Other surface charge-transfer processes may also be active,[20] but the magnitudes will almost certainly be less than the differences between a and b of Figure 4.

The matrix−metal LUMO-derived surface states acquire oscillator strength from the matrix and thus may be readily two-photon-ionized. Without this charge transfer, ionization is three-photon, which is less efficient. The SEM therefore predicts that ionization enhancement is dependent on the relative positions of the metal Fermi level and the LUMO, which can lead to dramatic differences in ionization efficiency for the same matrix on different metals.

As Figure 3 demonstrates, DHB exhibits strongly metal-dependent thin-sample MALDI yields consistent with this picture. From the level positions in Figure 4, SA could be expected to do so as well. It should be noted that such a level structure is a necessary condition for enhancement in the SEM, but not sufficient. The interaction with the metal must result in significant charge transfer across the boundary to the interfacial matrix, and matrix-excited states must not be excessively quenched at the surface. However, any material with an appropriate level structure is a candidate for the effect, and so can be tested.

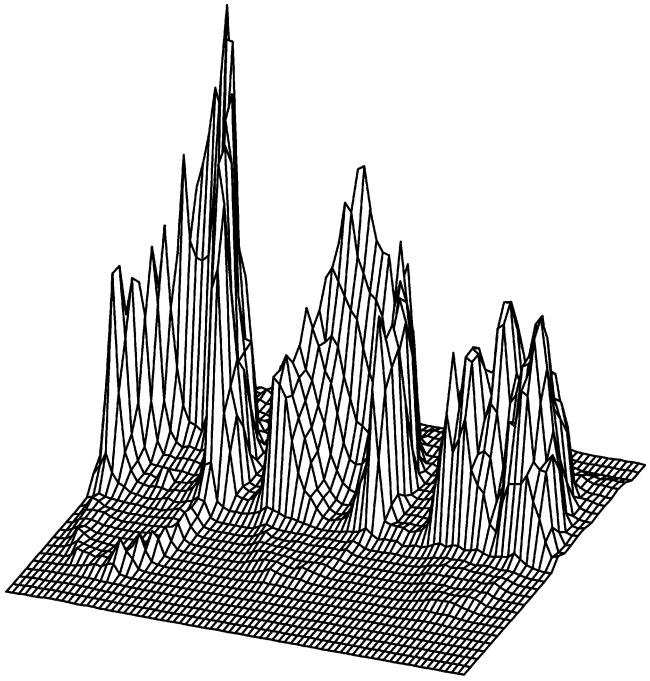

Figure 5. Electrosprayed SA MALDI spots on a stainless steel substrate which has been half-coated with 40 nm gold. The thinnest spot is on the right; the thickest, on the left. The spray times were 20, 10, and 5 s, from left to right. The images represent the sum of all SA matrix positive ions. The substantial signal enhancement of thin sample regions on steel is apparent, as is the much weaker effect on gold.

Figure 5 shows MALDI images of of thick and thin SA electrosprayed samples. The results are quite similar to those obtained for DHB matrix. The thin spots and thin edges of a thick sample exhibit strong enhancement on SS but only weak enhancement on gold. The magnitude of the relative enhancement is as large as or larger than that for DHB.

Having verified the SEM prediction of metal-dependent enhancement with SA, it is useful to investigate a different situation, in which no metal dependence should appear. As seen in Figure 4, HCCA matrix should behave very similarly on both SS and gold. From the level structure (LUMO below the Fermi level of both metals) there could be positive ion MALDI enhancement in both cases.

As shown in Figure 6, the signal level is indeed very similar on both metals. This is in strong contrast to thin DHB and SA samples. The thinnest edges show a strong enhancement, and all thin regions give a higher signal than the central thicker spot. All this is consistent with Figure 4 and ionization enhancement at the interface with both metals.

Negative Ions and Yield vs Metal. The PEC invokes the energy-dependent matrix electron capture cross-section to predict a metal dependence of the ions observed in the negative mode mass spectra. The photoelectron energy was found to be lower from gold than from steel,[3] and if this is near the capture maximum for a given matrix, anion production should be maximized, with associated loss of positive signal. This assumes a very dilute desorption plume, since otherwise electrons will be thermalized by multiple collisions and captured at the same rate regardless of their original emission energy. On the other hand a dense plume would seem to be needed for extensive recombination of positive and negative matrix ions.

On the basis of the energy dependence of the cross-section for electron capture to form $(DHB-H)^-$, the PEC predicts the

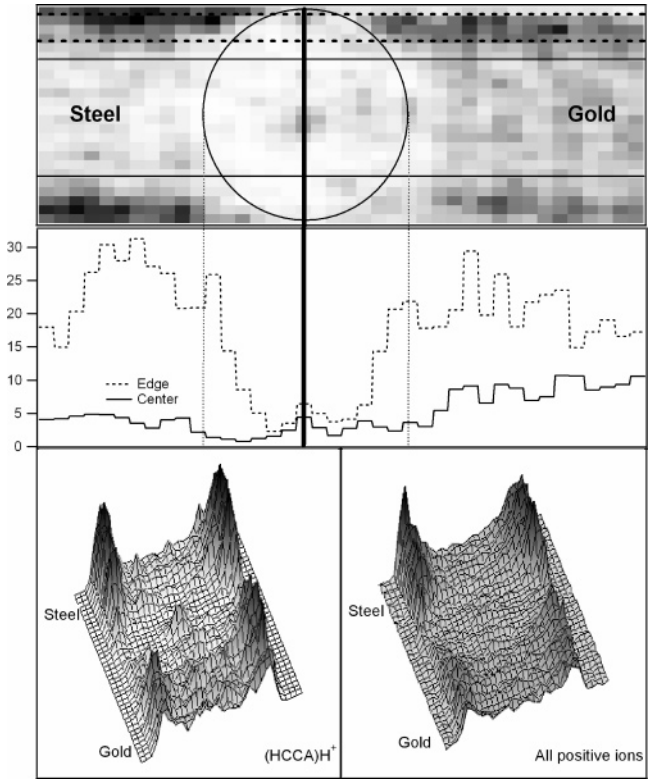

Figure 6. MALDI image of an electrosprayed HCCA track on a stainless steel substrate which has been half-coated with 40 nm gold. The MH^+ ion is shown; M^+ gave similar results. Darker pixels indicate a stronger signal. The thinner areas, where the sample was ablated to the metal interface, give enhanced signal on both gold and steel, by a similar amount. The thicker central spot (10 s spray time) shows reduced signal intensity. The thicker spot is approximately indicated by the circle in the upper image.

DHB matrix anion signal should be higher from the stainless steel than the gold substrate.[4] (This neglects the contribution of other dissociative capture channels at both higher and lower electron energies, at plumelike temperatures.[11]) Sinapinic acid similarly has its peak cross-section near or above 1 eV so should give the strongest anion signal on steel. The opposite is true for the HCCA matrix, which has a capture maximum at lower energy.[21] The SEM simply predicts that negative ion yield is enhanced if the positive yield is. It may be less enhanced than in positive mode, if the sample is not thick enough to capture all photoelectrons.

As seen in Figure 7, more DHB anions are indeed observed from a thin sample on SS than on gold. This is consistent with both models, as is the result for SA in Figure 8. The enhancement is largest for the thinnest regions, as found in positve mode.

The data for HCCA allow discrimination between the models. As seen in Figure 9, negative enhancement is similar on both metals, as for the positive ions. The thinnest regions show a slightly higher signal on steel than on gold. This is in constrast to the PEC prediction of more signal on gold. Again the thinnest edges give the largest effect, and the thicker spot is clearly the area of lowest ion yield.

Photoelectron Yield vs Laser Intensity. A large adsorbate-induced work function reduction is required in the PEC model to enable one-photon UV photoionization on matrix-coated metal. Work function reductions are well-known in surface science, but the magnitude required for one-photon photoemission at 355 nm is not. Taking into account the mean kinetic energies of the emitted electrons, reductions of around 1.5 (stainless) and 2 eV (gold) are required for this interpretation.

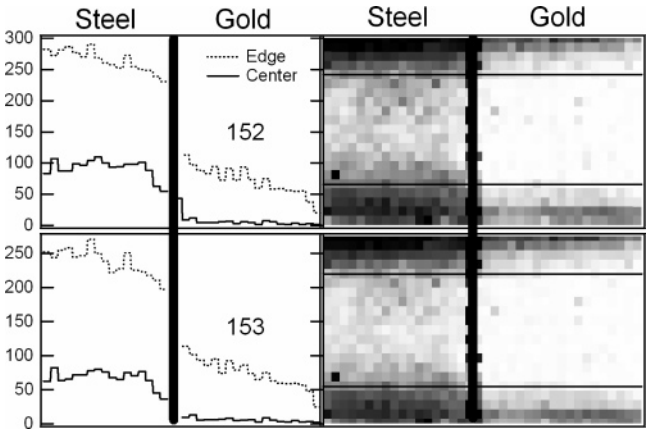

Figure 7. Negative ion MALDI images of a thin electrosprayed DHB track, spanning the boundary between a stainless steel and gold-coated steel substrate. Images of the two main DHB anions are shown, at m/z = 152 and 153. The signals are considerably stronger on the steel half, as is the positive ion signal. (Darker indicates higher signal or signal ratio.) Both the steel and gold sides exhibit more enhancement on the thinnest edges of the track, similar to the circular spots of Figure 3, but this is more pronounced for steel.

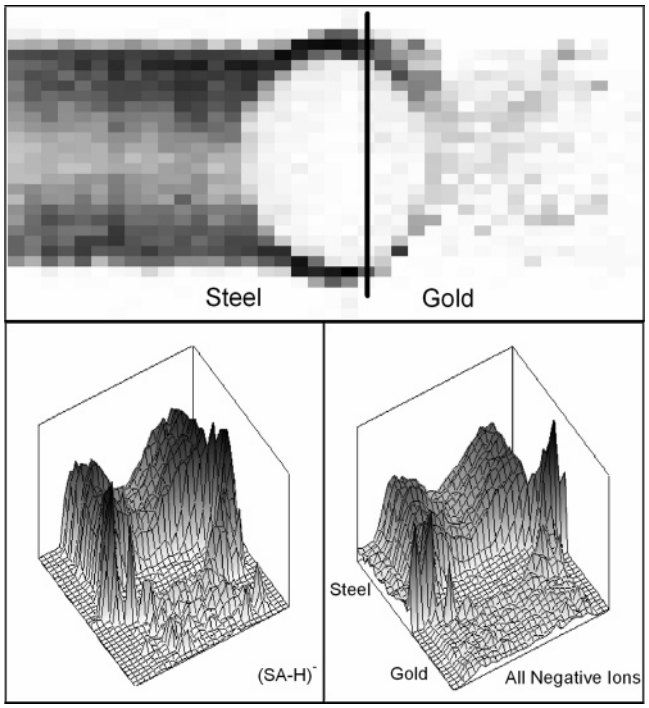

Figure 8. Negative ion ($(M-H)^-$) MALDI images of an electrosprayed SA track, spanning the boundary between a stainless steel and gold-coated steel substrate. Near the metal boundary, the spray was held stationary for 10 s to create a thicker region. The signals are considerably stonger on the thinner regions of the steel half than on gold. The thick central spot gave the weakest signal.

For surfaces which have been cleaned in ultrahigh vacuum prior to coating, reductions of over 1 eV have been found,[20,22] but not 2 eV. More relevant in the present context, metal surfaces prepared in air typically (but not always) exhibit distinctly smaller adsorbate-induced reductions, below 1 eV.[22] It would therefore be remarkable if multiple MALDI matrix substances were able to induce exceptionally large work function reductions on at least two metals. Direct evidence of work function reduction is therefore critical for the PEC. A linear electron yield vs laser intensity was proposed to provide this evidence.[3,4]

Capture of photoelectrons by SF_6 in an FT-ICR cell was used to determine the electron yield vs fluence for MALDI samples

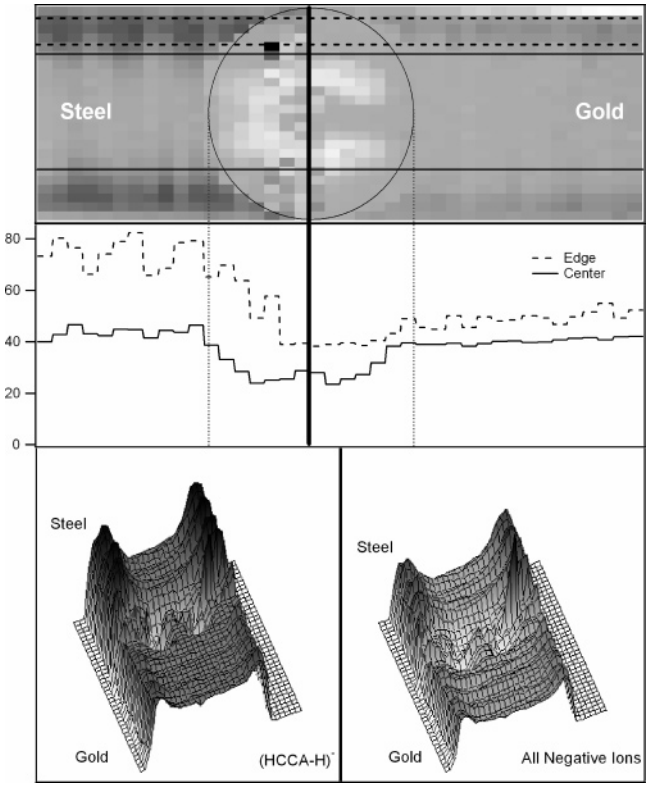

Figure 9. Negative ion ($(M-H)^-$) MALDI images of an electrosprayed HCCA track, spanning the boundary between a stainless steel and gold-coated steel substrate. Near the metal boundary, the spray was held stationary for 10 s to create a thicker region, as indicated by the circle in the upper image. The thick central spot gave the weakest signal, while the central thinner regions showed equal enhancement on both steel and gold. The thinnest edges exhibited a somewhat greater enhancement on steel than gold.

prepared by the dried-drop method.[3,4] The preparations were denoted as "thin" when macroscopic matrix crystals did not cover the whole substrate area. It was assumed that "blank" metal regions are coated with an active layer of matrix not apparent by optical inspection. The 355 nm laser beam was weakly focused (0.9 mm) and randomly scanned across the sample. The electron yield is therefore a sum of yields from regions of widely varying thickness. The fraction of blank area was also uncontrolled. From comparison with thicker and blank samples, it was proposed that most electrons could arise from the thinnest regions of the "thin" samples.

Electron yields from this method for 2,5-dihydroxybenzoic acid on steel, as reported in refs 3 and 4, are plotted in Figure 10. The lowest fluence measurements exhibit less scatter than the later higher fluence data. The uncertainties in the latter make connecting the data sets problematic, but they were scaled to meet at the overlapping points.

Comparing the data with the linear fit that passes through the origin to the data, it is apparent that there is some upward curvature in the low-fluence regime. At higher fluences, the data first lie above, then below, the best fit line. Downward curvature can be inferred, though the scatter is large. A linear fit to these data would not appear to fully reflect the observed trends.

The SEM has been cast into differential equations which can be numerically integrated.[5,14] The ionization step is either photoexcitation from the first electronic excited state or pooling of two singly excited molecules to yield one ion and a ground-state molecule.[14] For gold it is energetically three-photon, so a higher intermediate state is involved, as for the bulk matrix.[23,24]

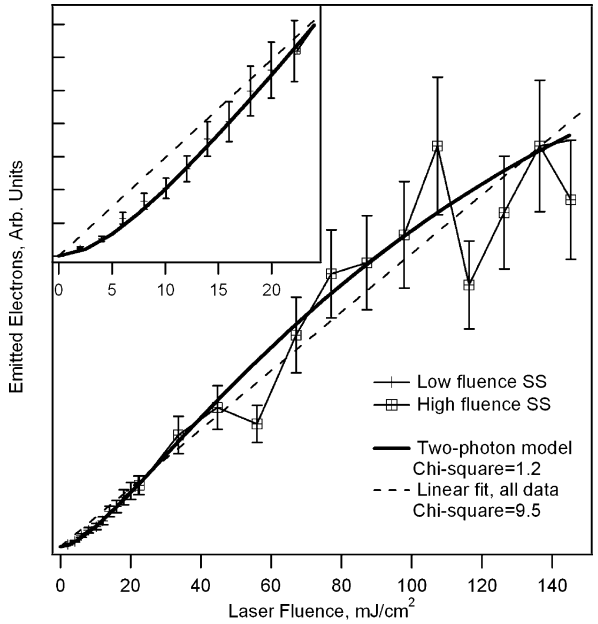

Figure 10. Electron emission data from DHB dried-drop samples on stainless steel, adapted from refs 3 and 4. The high-fluence measurements have been scaled to match the earlier low-fluence data at the point of overlap near 20 mJ/cm^2. Both a linear fit to the data (PEC model, dashed line) and the curve calculated from the SEM model (thick line) are shown. The inset shows the low-fluence range. The SEM is a much closer match to the data than a simple line, as reflected in the χ^2 parameter.

The parameters for DHB were derived from the quantitative MALDI model of refs 23 and 24. The absorption coefficients for the S_0-S_1 and S_1-ion transitions were 1.5×10^{-17} and 2×10^{-18} cm^2. The S_1 decay time including radiative and nonradiative components was 1 ns. The S_1-S_1 pooling rate was 7×10^9 s^{-1}.

As previously shown, this model matches the low-fluence stainless electron emission data for 2,5-dihydroxybenzoic acid extremely well.[14] Figure 10 shows that the match is also equally good in the high-fluence regime. The overall χ^2 value for the SEM model is about 8 times better than for the linear fit of the PEC model. The functional form of the SEM result is not quadratic because the two-photon process is sequential, not simultaneous, and because pooling contributes to ionization.

The SEM process describes the photoelectron data much better than a one-photon PEC process. These data cannot be taken to support large work function reductions for matrix-coated metal substrates.

Potential Instrumental Effects on MALDI Mass Spectra. As noted previously,[5] in a time-of-flight instrument we have found that thin dried-drop samples do not give significant metal substrate enhancement. It is possible that the type of mass spectrometer used is responsible for some of the discrepancies in reported thin sample results. In particular, the in-magnet MALDI source of refs 3 and 4 may be subject to effects not found using TOF sources. In the strong magnetic field, ions of both polarities as well as electrons will be constrained to move along the same field lines. Axial electrostatic trapping fields eventually separate positively and negatively charged species along these lines, but for a time they will be confined to a common cylindrical region. This is in strong contrast to a TOF source, where both neutrals and ions expand axially and radially away from the laser spot, reducing their interaction probability.

Factors Affecting Thin Sample Ion Yield and Practical Consequences. The present results were obtained with unusually

thin samples, and considerable effort was made to ensure that homogeneous, uniform films were produced. This required careful adjustment and control of the electrospray conditions. Only films giving strong colored interference fringes were found to give reproducible results. If the spray became unstable in any way, especially if filaments appeared, inconsistent results were obtained. This is attributed to the porous structures observed on microscopic inspection. Sometimes macroscopic cresecent structures were also observed, particularly with SA matrix. These samples did not give reproducible MALDI images.

The laser intensity was also found to have a significant effect on the relative SS/gold intensity ratios from transparent samples. Higher intensities tended to reduce the advantage of steel, but not eliminate it. This is partly an artifact, since after the sample is ablated to the metal, no further signal can be observed, but the results were averaged over all laser shots. Nevertheless, further investigation of the fluence dependence of thin sample yields appears warranted. Until this is better studied, those wishing to exploit thin sample enhancements should use lower laser intensities if maximum signal improvement is desired.

Samples as thin as studied here are not routinely used for MALDI. No doubt this is largely because little advantage has been perceived for spray methods over the convenient dried-droplet method. For DHB this is also partly because this matrix has a nonnegligible vapor pressure, limiting the lifetime of samples in the vacuum to a few hours. Nevertheless the present results and the drilling experiments of ref 5 show that it should be highly useful in practice to prepare thin MALDI samples and to ablate them down to a metal substrate, at least for the three matrixes investigated here. For DHB and SA the substrate should be SS, for HCCA gold is equally efficacious. The potential of other matrixes for similar enhancements can be estimated by considering the IP and first absorption band positions, compared to the metal Fermi level, as in Figure 4.

Conclusions

The ionization characteristics of thin MALDI matrixes on metal substrates were examined for three matrixes and two metals. Homogeneous electrosprayed samples were studied by imaging mass spectrometry across a stainless steel−gold boundary. Thin sample ionization enhancement in positive and negative modes was observed for all three. The enhancement was much larger on stainless steel than on gold for DHB and SA. HCCA gave similar signal on SS and gold.

Photoelectron emission from DHB-coated stainless steel was also reexamined. For DHB, the two-photon ionization model gave a clearly superior reproduction of the data in all fluence ranges, compared to the one-photon linear model.

These data are fully consistent with the surface matrix ionization enhancement model but are almost entirely inconsistent with the photoelectron capture model. We find no evidence for an unprecedentedly large work function reduction due to matrix adsorption, nor one-photon ionization of interfacial matrix. Two-photon ionization including sequential excitation, exciton hopping, and pooling, appears to be a better explanation for characteristics of thin sample MALDI performance.

The use of thin samples on metal substrates appears to be a useful analysis technique. Even if extremely thin samples are not used, it remains advantageous to ablate to the metal interface to take advantage of the increased signal obtained from the last layers. The metal sustrate should be chosen to be compatible with the matrix used.

References and Notes

(1) Frankevich, V.; Knochenmuss, R.; Zenobi, R. *Int. J. Mass Spectrom.* **2002**, *220*, 11−19.
(2) Frankevich, V.; Zhang, J.; Dashtiev, M.; Zenobi, R. *Rapid Commun. Mass Spectrom.* **2003**, *17*, 2343−2348.
(3) Frankevich, V.; Zhang, J.; Friess, S. D.; Dashtiev, M.; Zenobi, R. *Anal. Chem.* **2003**, *75*, 6063−6067.
(4) Dashtiev, M.; Frankevich, V.; Zenobi, R. *J. Phys. Chem. A* **2006**, *110*, 926−930.
(5) McCombie, G.; Knochenmuss, R. *J. Am. Soc. Mass Spectrom.* **2006**, *17*, 737−745.
(6) Hensel, R. R.; King, R. C.; Owens, K. G. *Rapid Commun. Mass Spectrom.* **1997**, *11*, 1785−1793.
(7) Axelsson, J.; Hoberg, A.-M.; Waterson, C.; Myatt, P.; Shield, G. L.; Verney, J.; Haddelton, D. M.; Derrick, P. J. *Rapid Commun. Mass Spectrom.* **1997**, *11*, 209−213.
(8) Karbach, V.; Knochenmuss, R. *Rapid Commun. Mass Spectrom.* **1998**, *12*, 968−974.
(9) Lin, Q.; Knochenmuss, R. *Rapid Commun. Mass Spectrom.* **2001**, *15*, 1422−1426.
(10) Asfandiarov, N. L.; Pshenichnyuk, S. A.; Forkin, A. I.; Lukin, V. G.; Fal'ko, V. S. *Rapid Commun. Mass Spectrom.* **2002**, *16*, 1760−1765.
(11) Pshenichnyuk, S. A.; Asfandiarov, N. L.; Fal'ko, V. S.; Lukin, V. G. *Int. J. Mass Spectrom.* **2003**, *227*, 281−288.
(12) Pshenichnyuk, S. A.; Asfandiarov, N. L.; Fal'ko, V. S.; Lukin, V. G. *Int. J. Mass Spectrom.* **2003**, *227*, 259−272.
(13) Karas, M.; Glückmann, M.; Schäfer, J. *J. Mass Spectrom.* **2000**, *35*, 1−12.
(14) Knochenmuss, R. *Anal. Chem.* **2004**, *76*, 3179−3184.
(15) Allwood, D. A.; Dreyfus, R. W.; Perera, I. K.; Dyer, P. E. *Rapid Commun. Mass Spectrom.* **1996**, *10*, 1575−1578.
(16) Horneffer, V.; Dreisewerd, K.; Lüdemann, H.-C.; Hillenkamp, F.; Laege, M.; Strupat, K. *Int. J. Mass Spectrom.* **1999**, *185*−*87*, 859.
(17) Setz, P.; Knochenmuss, R. *J. Phys. Chem. A* **2005**, *109*, 4030−4037.
(18) Stoeckli, M.; Staab, D.; Staufenbiel, M.; Wiederhold, K. H.; Signor, L. *Anal. Biochem.* **2002**, *311*, 33−39.
(19) Gorshkov, M. V.; Frankevich, V. E.; Zenobi, R. *Eur. J. Mass Spectrom.* **2002**, *8*, 67−69.
(20) Ishii, H.; Sugiyama, K.; Ito, E.; Seki, K. *Adv. Mater.* **1999**, *11*, 605−625.
(21) Pshenichnyuk, S. A.; Asfandiarov, N. L. *Eur. J. Mass Spectrom.* **2004**, *10*, 477−486.
(22) Seki, K.; Hayashi, N.; Oji, H.; Ito, E.; Ouchi, Y. IP reduction organic on metals. *Thin Solid Films* **2001**, *393*, 298−303.
(23) Knochenmuss, R. *J. Mass Spectrom.* **2002**, *37*, 867−877.
(24) Knochenmuss, R. *Anal. Chem.* **2003**, *75*, 2199.
(25) Hoteling, A. J.; Nichols, W. F.; Giesen, D. J.; Lenhard, J. R.; Knochenmuss, R. *Eur. J. Mass Spectrom.*, in press.
(26) Allwood, D. A.; Dreyfus, R. W.; Perera, I. K.; Dyer, P. E. *Appl. Surf. Sci.* **1997**, *110*, 154−157.